Structure of Alginate Gels: Interaction of Diuronate Units with Divalent Cations from Density Functional Calculations

ARTICLE *in* BIOMACROMOLECULES · MAY 2012

Impact Factor: 5.75 · DOI: 10.1021/bm300420z · Source: PubMed

5 AUTHORS, INCLUDING:

Velina K. Markova
Sofia University "St. Kliment Ohridski"
3 PUBLICATIONS **23** CITATIONS
SEE PROFILE

Mike Robitzer
Ecole Nationale Supérieure de Chimie de Mon…
42 PUBLICATIONS **699** CITATIONS
SEE PROFILE

Françoise Quignard
French National Centre for Scientific Research
101 PUBLICATIONS **2,394** CITATIONS
SEE PROFILE

Tzonka Mineva
Institut Charles Gerhardt
89 PUBLICATIONS **983** CITATIONS
SEE PROFILE

Article

pubs.acs.org/Biomac

Structure of Alginate Gels: Interaction of Diuronate Units with Divalent Cations from Density Functional Calculations

Pierre Agulhon, Velina Markova, Mike Robitzer, Françoise Quignard, and Tzonka Mineva*

Institut Charles Gerhardt Montpellier, UMR 5253 CNRS-UM2-ENSCM-UM1, Matériaux Avancés pour la Catalyse et la Santé, ENSCM, 8 rue de l'Ecole Normale, 34296 Montpellier cedex 5, France

Supporting Information

ABSTRACT: The complexation of (1→4) linked α-L-guluronate (G) and β-D-mannuronate (M) disaccharides with Mg^{2+}, Ca^{2+}, Sr^{2+}, Mn^{2+}, Co^{2+}, Cu^{2+}, and Zn^{2+} cations have been studied with quantum chemical density functional theory (DFT)-based method. A large number of possible cation−diuronate complexes, with one and two GG or MM disaccharide units and with or without water molecules in the inner coordination shells have been considered. The computed bond distances, cation interaction energies, and molecular orbital composition analysis revealed that the complexation of the transition metal (TM) ions to the disaccharides occurs via the formation of strong coordination-covalent bonds. On the contrary, the alkaline earth cations form ionic bonds with the uronates. The unidentate binding is found to be the most favored one in the TM hydrated and water-free complexes. By removing water molecules, the bidentate chelating binding also occurs, although it is found to be energetically less favored by 1 to 1.5 eV than the unidentate one. A good correlation is obtained between the alginate affinity trend toward TM cations and the interaction energies of the TM cations in all studied complexes, which suggests that the alginate affinities are strongly related to the chemical interaction strength of TM cations−uronate complexes. The trend of the interaction energies of the alkaline earth cations in the ionic complexes is opposite to the alginate affinity order. The binding strength is thus not a limiting factor in the alginate gelation in the presence of alkaline earth cations at variance with the TM cations.

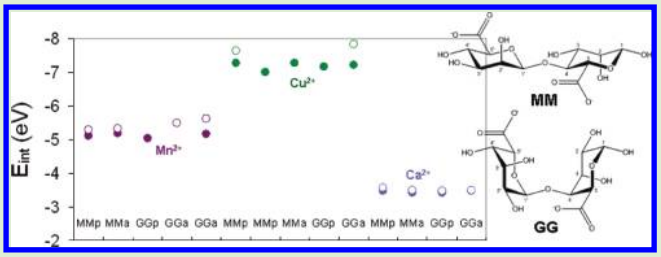

INTRODUCTION

Alginate is a polysaccharide of (1→4) linked α-L-guluronate (G) and β-D-mannuronate (M) (Scheme 1); it is a natural copolymer in the brown seaweeds with a nonregular blockwise arrangement between the G and M units.[1−3] The presence of di- and trivalent metal ions in water cause the formation of strong and rigid ordered structures, the hydrogels. This property is the basis of both biological and industrial applications of alginates. Many works have been accumulated in an attempt to understand the gel strengths and stabilities with varying the ion concentration, the nature of metal ion, and the pH of the solvent.[4−11] A different affinity of metal ions was established for the G and M homopolymers by using circular dichroism,[12−14] calorimetry,[15] and dilatometry[16] methods. The G-rich chains exhibit high affinity toward Ca^{2+}, Ba^{2+}, and Sr^{2+} ions at low concentration contrary to the M-rich or alternating M and G blocks.[17] This difference is explained with the secondary structure of alginates. The diaxial bond in a homopolymeric chain of guluronates determines a curved fiber structure forming cavities, which facilitates the metal cation accommodation inside these negative cavities (Scheme 1). The most accepted model giving a simple picture of the Ca^{2+}−guluronates interaction is the so-called "egg-box",[12,18] where one Ca^{2+} binds to G units in two alginate chains. Other possible structures have been also suggested based on the analysis of the X-ray[19] and NMR spectroscopy data.[20] A selective binding of the earth-alkaline ions to the guluronates was concluded from the dialysis experiments.[7,21,22] At a high concentration, the metal ions bind also to the M units.

The first step of the alginate gelation processes is the metal complexation to the carboxylates. Except for Ca^{2+}−alginate interactions, little is known about the binding of various metal ions, the resulting local carboxylate structures, and their relation to the chain conformations. Theoretical studies, performed with classical force field methods,[23,24] corroborate the egg-box model and the preference of Ca^{2+} to G-rich polymers. On the experimental basis, the FT-IR spectroscopy has been applied as local probe to resolve the binding types of TM divalent ions−alginate complexes.[25,26] The idea is to explore the empirically established relationship between the type of binding of metal cations with the carboxylates and the separation between the symmetric and asymmetric stretching vibrational bands, $\Delta\nu(COO^-)$, of the carboxylate groups.[27] This empirical relation was also quantified using ab initio calculations.[28] The considered types of metal−alginate coordinations are those suggested by Nakamoto[27] for one metal per carboxyl group. These binding modes are shown in Scheme 2 as follows: (a) an

Received: March 17, 2012
Revised: May 4, 2012
Published: May 9, 2012

Scheme 1. Schematic Presentation of Linked α-L-Guluronate (G) and β-D-Mannuronate (M) isomers

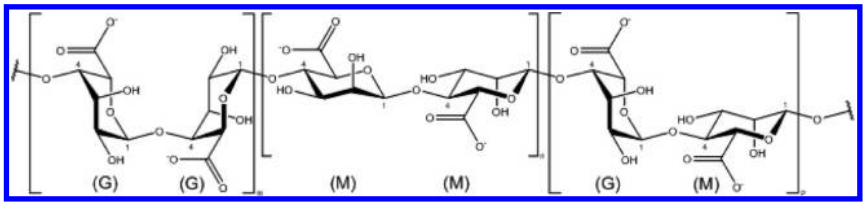

ionic or uncoordinated type; (b) unidentate type; (c) bidentate chelating type; and (d) pseudo-bridging unidentate type.

Scheme 2. Metal-Carboxylate Binding Modes for One Metal Per Carboxylic Group As Proposed by Nakamoto[27]

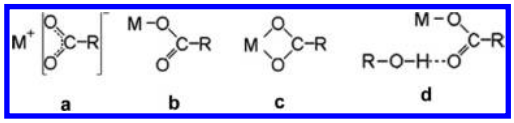

Following this FT-IR analysis Papageorgiou et al.[26] concluded that the pseudo-bridging unidentate mode (Scheme 2d) is the most probable binding in the polyguluronate−metal complexes, whereas the bidentate bridging coordination, that is, two metal cation per COO^- unit (not shown in Scheme 2), in the polymannuronate−metal complex was established. The latter findings contradict the previous FT-IR analysis, proposing the bidentate chelating coordination mode[25] (Scheme 2c). It was therefore suggested[26] that the FT-IR spectroscopy cannot be used as the only tool, providing sufficient information about local structures of metal−alginate complexes.

In the present work, we address questions related to metal complexations to carboxylates, the type of binding, and chemical interactions of cation−alginate complexes by applying first-principle computational methods. Our results showed unambiguously that there is only electrostatic interaction in the alkaline-earth (AE) cations−uronate units, whereas the complexes of the TM cations are formed due to strong covalent-coordination bonds.

MODELS AND METHODS

Models. In the present work, we have explored a large number of structures, formed due to complexations of Mg^{2+}, Ca^{2+}, Sr^{2+}, Mn^{2+}, Co^{2+}, Cu^{2+}, and Zn^{2+} with alginates chains. In all models, only homoisomeric two uronate (U) units have been considered. The models represent structures used to study in detail the chemical interactions and possible types of bindings between divalent metal cations and U units as a function of metal chemical nature and alginate M and G isomers.

The choice of the initial conformations of the G and M disaccharides is based on the conformational screening performed with restricted Hartree−Fock (HF) method. As already demonstrated,[19,24,29] the polysaccharides conformations depend mainly on the two torsion angles about the glycosidic bond, ϕ (O5′−C1′−O4−C4) and ψ (C1′−O4−C4−C5) (Figure 1). The HF (ϕ, ψ) potential energy map in a window of 8 kcal/mol is drawn in Figure 1 together with the alginate two units chain. The results show several distinct low-energy regions within 1 kcal/mol for both GG (four conformers within 1 kcal/mol) and MM (three conformers within 1 kcal/mol) units. The (ϕ, ψ) torsion angles for the four most stable guluronic acid conformers are (60°; 250°); (20°; 280°); (320°; 300°); are (280°; 180°). The most favored conformers of MM units are those with (ϕ, ψ) torsion angles of (347°; 304°); (307°; 344°); and (267°; 24°). The existence of several low-energy regions on the potential maps, revealed relatively largely accessible conformational spaces for both (1→4) diaxial or (1→4) diequatorial glycosidic linkage in a window of 1 kcal/mol. The HF method yielded larger conformational space than that obtained from the previous molecular mechanics or molecular dynamics methods,[24,29] where the torsional potentials depend also on a parameter set, remaining unchanged in the self-consistent field calculations.

All complex structures we have considered were built from the most stable MM and GG conformers with the two COO^- groups oppositely

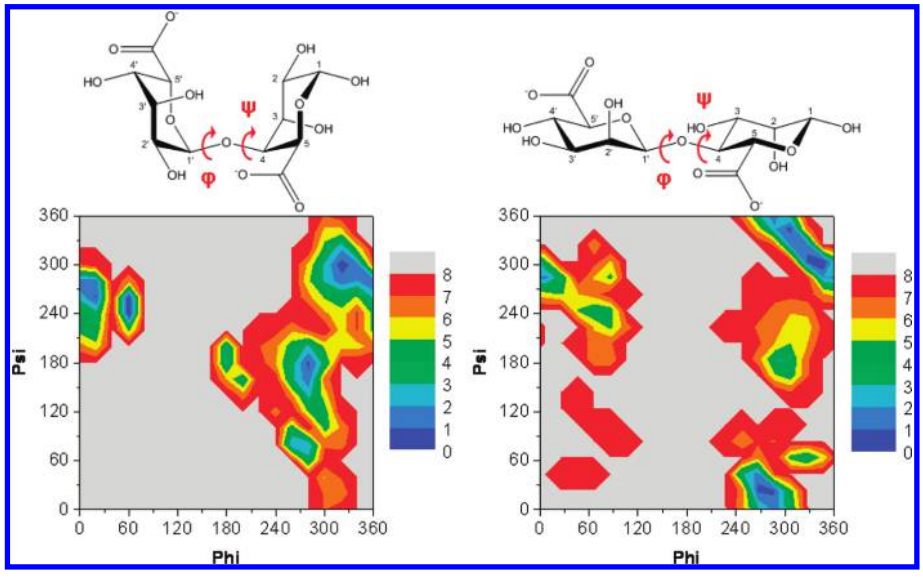

Figure 1. Potential energy maps for the GG and MM disaccharides computed with Hartree−Fock method. The potential energy map consists of the conformations with relative energies within 8 kcal/mol.

dx.doi.org/10.1021/bm300420z | Biomacromolecules 2012, 13, 1899−1907

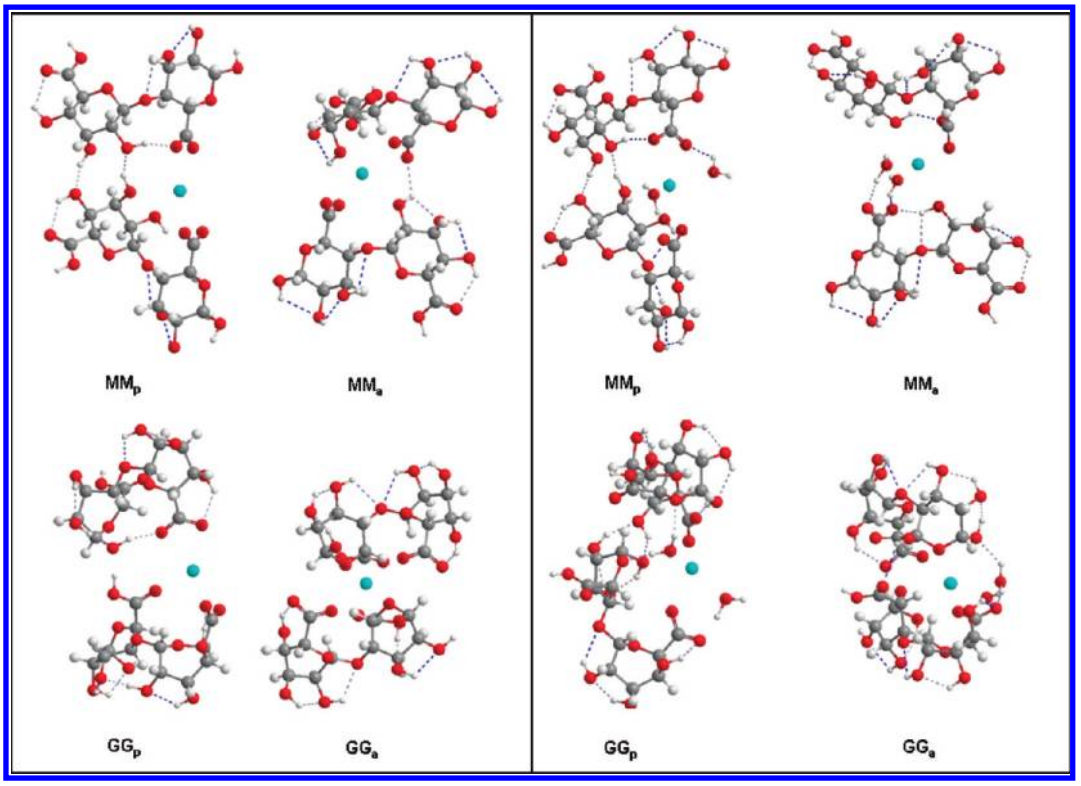

Figure 2. Optimized structures of Sr^{2+}–disaccharide complexes without water molecules (left panel) and with water molecules (right panel). The atoms are represented with balls colored by atom type as follows: red for oxygen, gray for carbon, white for hydrogen, and cyan for strontium. The oxygens, participating in the ionic coordination bonds, are indicated by "O". The indices "p" and "a" denote, respectively, the parallel and antiparallel orientations of the disaccharide units.

displaced (Figure 1). These structures were subsequently fully optimized with DFT. The optimized (ϕ, ψ) torsion angles in GG and MM units are (305°; 292°) and (274°; 344°), respectively. Because the metal-to-alginate complexation is expected to occur preferably via a metal binding to carboxylate oxygen,[30] we have considered as the smallest model, representing the metal–alginate gelation, two disaccharide units from two alginate chains complexing to one metal center. Moreover, new thermogravimetry measurements confirmed one divalent ion per two COO^- groups.[31] For this reason, models with two metal ions, binding to the same COO^- site, were not studied. Parallel (p) and antiparallel (a) chain orientations were considered. For comparison, complexes consisting of one disaccharide (two U units) were also computed. The structures with two disaccharides modeling two alginate chains are labeled throughout the text as 2-DC, and those with one disaccharide, representing one truncated alginate chain, are labeled as 1-DC. Complexes with water molecules in the first- or second-coordination shells have also been studied.

Full geometry optimization has been undertaken for all models, and the interaction energies of the metal cations and the U-units were computed for the minimum energy structures.

The polarization effect of water, without explicit solvent molecules, was examined with polarized continuum method (PCM),[32] where the water medium is represented by its bulk dielectric constant. The energy minimization procedure with the PCM was carried out. The studies were performed for Ca^{2+}, Cu^{2+}, and Mn^{2+} 2-DC complexes, and the results showed no structural variations due to the polarization of water medium.

Methods. The computational method employed is based on the density functional theory (DFT) using the Perdew–Burke–Ernzerhof's 1996 (PBE) exchange-correlation functional approximation.[33] The Gaussian09[34] program was employed for the conformational scanning of GG and MM disaccharides and for the calculations with the PCM scheme. The geometry optimizations of the studied complexes were carried out with the deMon2k program.[35,36]

Triple-ζ basis sets were used for the C, O, and H atoms and double-ζ bases plus polarization[37] for metal cations. Automatically generated auxiliary functions up to $l = 2$ (for the metal atoms) and 3 (for H, C, and O atoms) were used for fitting the density.[38] An empirical London dispersion energy was added to the total energy and to the energy gradients in the geometry optimization calculations.[39] The London dispersion contribution to the total energies amounts to 3 to 3.6 eV in all studied complexes.

A quasi-Newton method in internal redundant coordinates with analytical energy gradients was used for the structure optimizations.[40] The convergence was based on the Cartesian gradient and displacement vectors with thresholds of 10^{-4} a.u. The interaction energies were corrected for the basis set superposition error, which was computed to be on the order of 1.5 eV in all of the cases.

RESULTS

In this section, the geometrical and energetic results for the minimum energy structures of cation complexes with two disaccharides, 2-DC, will be presented. The divalent cations–alginate interaction in the structures with one disaccharide, 1-DC, closely resembles that in the 2-DC complexes, with the difference that it is necessary to add water molecules in the first-coordination shell in the 1-DC complexes to saturate the coordination bonds. Details of the structural (geometric and energetic) results for the 1-DC structures are reported in the Supporting Information (SI), sections SI1 and SI2.

Alkaline Earth Cations–Diuronate Complexes. The complexation of Mg^{2+}, Ca^{2+}, and Sr^{2+} to one or two disaccharides leads to very similar structures for the three ions. As a representative case, we have reported in Figure 2 the optimized Sr^{2+}–alginate complexes with two chains. The alkaline earth ions (M^{2+}) form five or six short ionic bonds with the carboxyl and hydroxyl oxygens. As expected, the

dx.doi.org/10.1021/bm300420z | Biomacromolecules 2012, 13, 1899–1907

$M^{2+}\cdots O$ distances increase with the ionic radius: $Mg^{2+} < Ca^{2+} < Sr^{2+}$. The averaged $Mg^{2+}\cdots O$, $Ca^{2+}\cdots O$, and $Sr^{2+}\cdots O$ distances are 2.156, 2.471, and 2.610 Å, respectively. The $Ca^{2+}\cdots O$ averaged distances are in good agreement with previously studied Ca^{2+}−alginate interactions using force-field computational methods.[22,23] In these works, six short $Ca^{2+}\cdots O$ bond lengths of ∼2.4 Å were reported.

The complex topologies are characteristic for the uronate isomer and their mutual orientation. The parallel displaced MM chains are characterized by four $COO^{-}\cdots M^{2+}$ and two $HO\cdots M^{2+}$ ionic bonds (Figure 2). For the antiparallel MM orientations, we obtained three $COO^{-}\cdots M^{2+}$ and three $HO\cdots M^{2+}$ ionic bonds. It is interesting to note that the M^{2+}−MM_p interaction in the structures with parallel chains leads to the formation of two interchain H-bonds of similar lengths (of 1.6 and 1.7 Å) for the three alkaline earth ions, which is not the case if an antiparallel orientation is considered. These two intermolecular chain H bonds have nearly negligible effect on the stabilization of the "parallel" complexes. In the case of M^{2+}-GG_a structures, the alginates orient in the way to place also the ring oxygen close to the metal ion, thus forming two bonds with O5, two with COO^{-}, and two with OH groups. In all cases, the bond lengths decrease from $O5\cdots M^{2+}$, to $HO\cdots M^{2+}$, to $COO^{-}\cdots M^{2+}$ by about 0.1 to 0.2 Å. In the carboxylates with parallel disaccharides, one of the uronate dimer rotates so that its second COO^{-} group turns toward the cation, which becomes surrounded by three closely spaced carboxylate groups (Figure 2) and is characterized with five short distances in difference from the other complexes having six short $M^{2+}\cdots O$ bonds.

The uronate dimer conformations undergoes some changes when forming carboxylates; however, the characteristic (ϕ,ψ) angles (Figure 1) remain in most of the structures close to their values in the optimized U dimers. For instance, the ϕ angle is ∼310° in the 2-DC Sr^{2+} structures with two GG disaccharides, and the ψ angle is between 260 and 250°. A larger variation is observed for the complexation with MM isomers. In the MM_a structures, the (ϕ,ψ) values are (273°; 208°) and (266°; 255°), and in MM_p the values are (267°;131°) and (267°; 235°).

The minimum energy structures of the hydrated 2-DC models including two H_2O molecules in the first coordination shell are also presented in Figure 2 (right panel). Six short ionic bonds between the metal center and the ligands are obtained, except in the MM_p complexes being formed by seven short ionic bonds. Coordination numbers of Ca^{2+}−carbohydrate complexes in the presence of water have been reported to vary between 7 and 9.[41]

In all structures, two of the short $M^{2+}\cdots O$ distances are with water's oxygens. The averaged $M^{2+}\cdots O$ distances remain very similar as in the water-free structures, and their averaged lengths are, respectively, 2.178, 2.483, and 2.662 Å in the Mg^{2+}, Ca^{2+}, and Sr^{2+}- complexes. Ca^{2+}-O-averaged distance matches very well the value of 2.48 Å obtained from the analysis of geometrical parameters of a large set of hydrated Ca^{2+}−carbohydrate complexes.[41]

The interaction energies, E_{int}, of the alkaline-earth ions per bond were computed from the following equation

$$E_{int} = \frac{1}{m}[E_{complex} - (2{*}E_{monomer} + n{*}E_{H_2O} + E_{cation})]$$

where n is the number of water molecules and m is the number of bonds per cation in the complex. It is not surprising for the ionic compounds that E_{int} increases with the decrease in the ionic radius following the order:[42] $Mg^{2+} > Ca^{2+} > Sr^{2+}$. For a given ion, there is not a clear preference for the chain orientation and the type of the uronate units. (The E_{int} values are reported in Table SI3.1 in the Supporting Information.)

First-Row Transition-Metal Divalent Cations−Diuronate Complexes. The interaction among Mn^{2+}, Co^{2+}, Cu^{2+}, and Zn^{2+} and MM and GG uronates was studied assuming in the initial complex geometries all binding modes presented in Scheme 2 for one metal center. The unidentate and bidentate chelating types of binding were found in the optimized minimum energy complexes. Optimized minimum energy structures are shown in Figures 3-6 for Mn^{2+}, Co^{2+}, Cu^{2+}, and Zn^{2+}, respectively. The coordination number of Co^{2+} and Cu^{2+} is four, and that of Mn^{2+} and Zn^{2+} is five. The optimized TM−O bond distances are collected in Table SI3.2 in the Supporting Information.

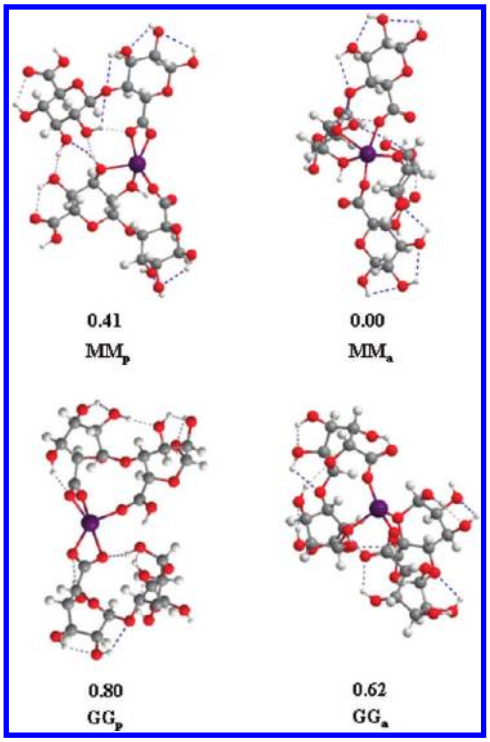

Figure 3. Optimized structures and relative energies in electronvolts of Mn^{2+}−disaccharide complexes. The atoms are represented with balls colored by atom type as follows: red for oxygen, gray for carbon, white for hydrogen, and violet for manganese. The indices "p" and "a" denote, respectively, the parallel and antiparallel orientations of the disaccharide units.

The relative energies with respect to the most stable structure for a particular TM cation are reported below each complex in Figures 3−6 as well. As it follows, the TM ions prefer the unidentate binding, which is obtained when considering antiparallel orientation between two MM dimers. In the parallel MM-chain configuration and in the GG structures, the transition-metal ions link in a unidentate type to one of the chains and in a bidentate type to the other one. A complete bidentate chelating binding to both disaccharides is found only in a Cu^{2+}−carboxylate (Figure 5) with the alginate chains in parallel mutual orientation. This structure is, however, the least stable one among the other Cu^{2+} complexes. The interaction of the uronate dimers with the TM cations causes different mutual displacements between both chains in relation

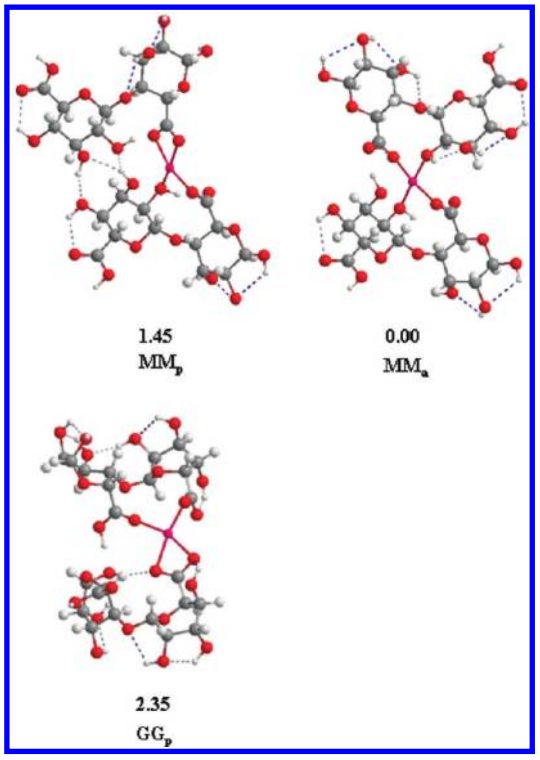

Figure 4. Optimized structures and relative energies in electronvolts of Co^{2+}−disaccharide complexes. The atoms are represented with balls colored by atom type as follows: red for oxygen, gray for carbon, white for hydrogen, and pink for cobalt. The indices "p" and "a" denote, respectively, the parallel and antiparallel orientations of the disaccharide units.

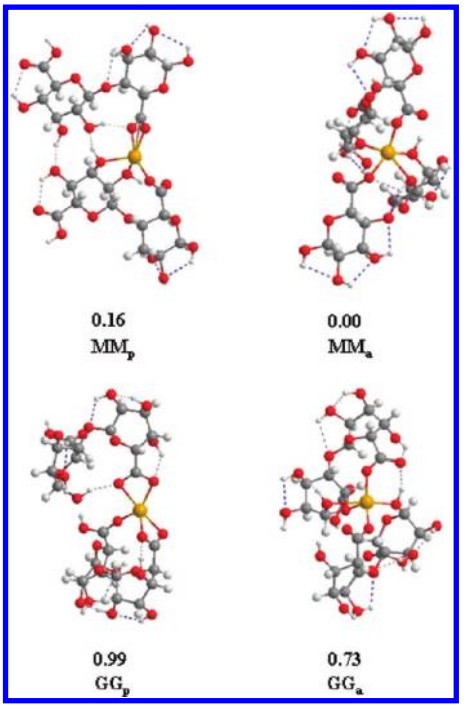

Figure 6. Optimized structures and relative energies in electronvolts of Zn^{2+}−disaccharide complexes. The atoms are represented with balls colored by atom type as follows: red for oxygen; gray for carbon, white for hydrogen, and yellow for zinc. The indices "p" and "a" denote, respectively, the parallel and antiparallel orientations of the disaccharide units.

to their M or G isomers, as it can be seen from a general inspection of the optimized structures. The complex topology also depends on the number of TM−O bonds, as deduced from the similarity between the Cu^{2+} and Co^{2+} complexes, and between the Mn^{2+} and Zn^{2+} structures. The interaction

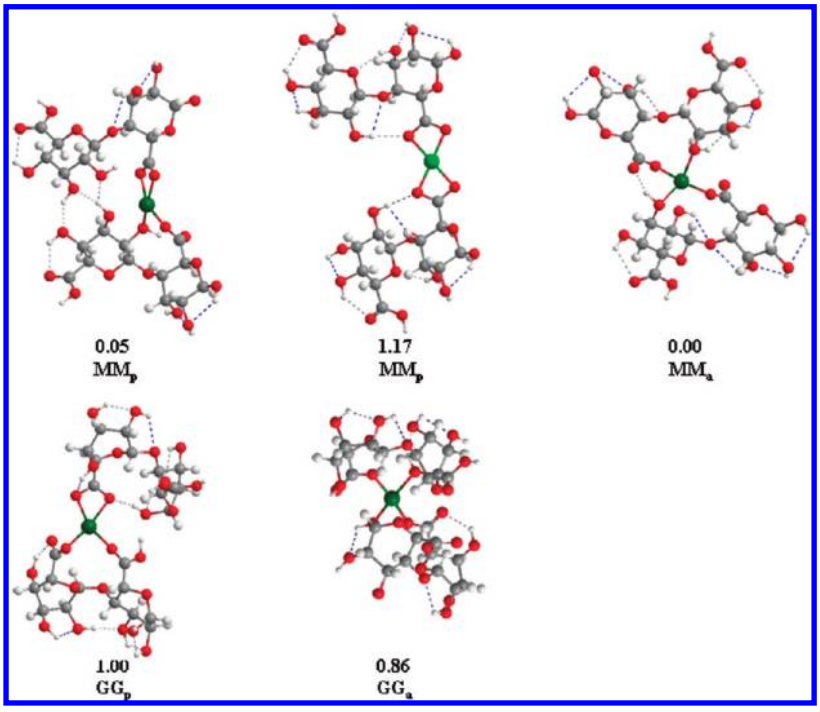

Figure 5. Optimized structures and relative energies in electronvolts of Cu^{2+}−disaccharide complexes. The atoms are represented with balls colored by atom type as follows: red for oxygen, gray for carbon, white for hydrogen, and green for copper. The indices "p" and "a" denote, respectively, the parallel and antiparallel orientations of the disaccharide units.

dx.doi.org/10.1021/bm300420z | *Biomacromolecules* 2012, 13, 1899−1907

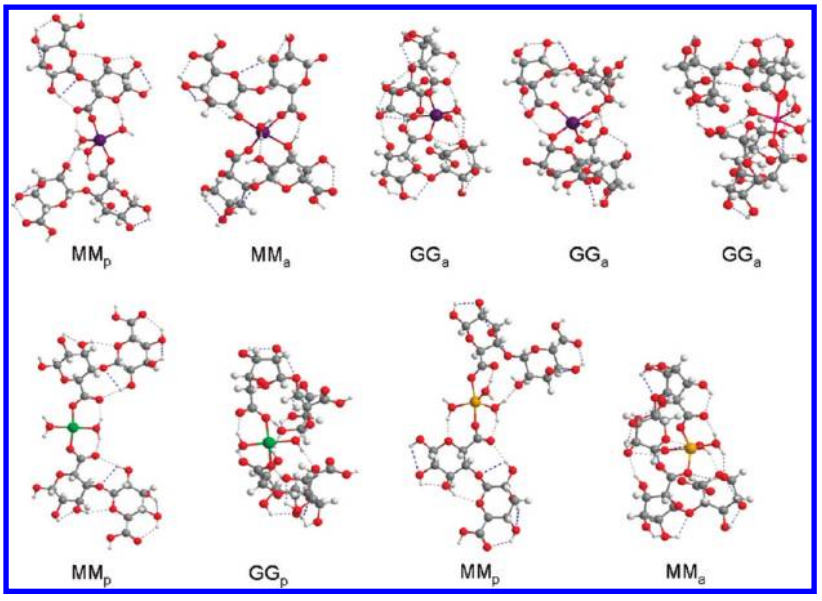

Figure 7. Optimized structures of transition metal − disaccharide complexes containing water molecules in the first coordination shell. The atoms are represented with balls colored by atom type as follows: red for oxygen, gray for carbon, white for hydrogen, violet for manganese, pink for cobalt, green for copper, and yellow for zinc. The indices "p" and "a" denote, respectively, the parallel and antiparallel orientations of the disaccharide units.

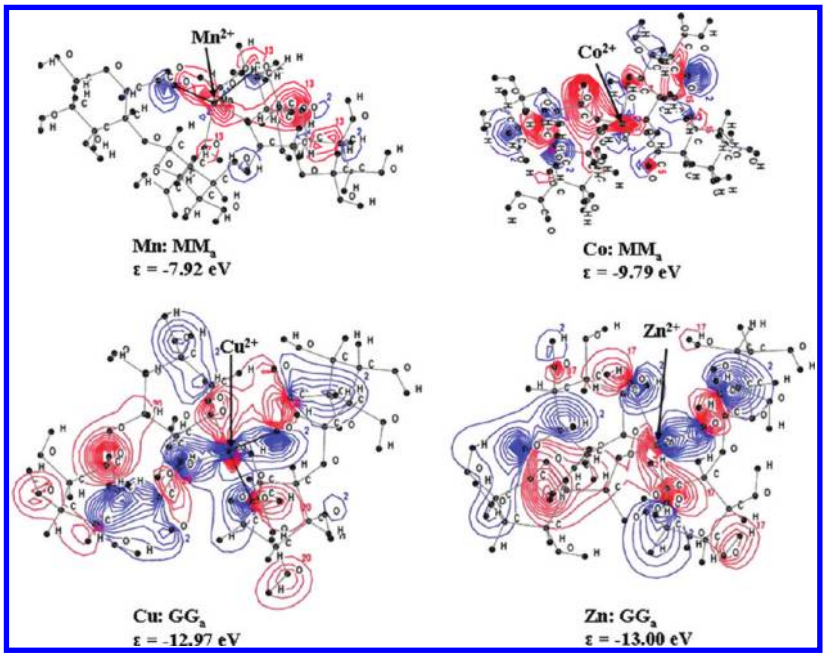

Figure 8. Plot of representative molecular orbitals predominantly composed from carboxyl and/or hydroxyl O_{2p} and 3d atomic orbitals in transition metal−diuronate complexes.

energies, calculated in the same way as for the alkaline earth ions, are reported in Table SI3.2 in the Supporting Information.Whatever the structure and the isomer of the uronate unit, the E_{int} has the highest value for Cu^{2+}, followed by Co^{2+}, Zn^{2+}, and Mn^{2+}, being only slightly smaller than for Zn^{2+} cation.

Water molecules in the first-coordination shells have been taken into account as well. In the water-containing carboxylate models, the TM ions always form shorter bond lengths with the water oxygen atoms compared with those with the COO^- and OH groups, similarly to the complexation with alkaline earth metals. Only the unidentate type of binding occurs if water is present. In either the hydrated or water-free complexes the TM−O distances are of comparable lengths. In Figure 7, the most stable water-containing structures are presented, and the range of the TM−O bonds as well as the TM interaction energies are also reported in Table SI3.2 in the Supporting Information. The parallel orientation between the GG chains and water in the first-coordination shell did not result in stable complexes in difference from the antiparallel displacements. This was not observed for the MM units.

The effect of varying water molecules in the first-coordination shell has also been studied for Mn^{2+}−GG_a. The cations bind in a unidentate type to the two COO^- if the other bonds are saturated by water. By removing H_2O molecules, the TM ion coordination shell starts to be saturated by binding to

dx.doi.org/10.1021/bm300420z | *Biomacromolecules* 2012, 13, 1899−1907

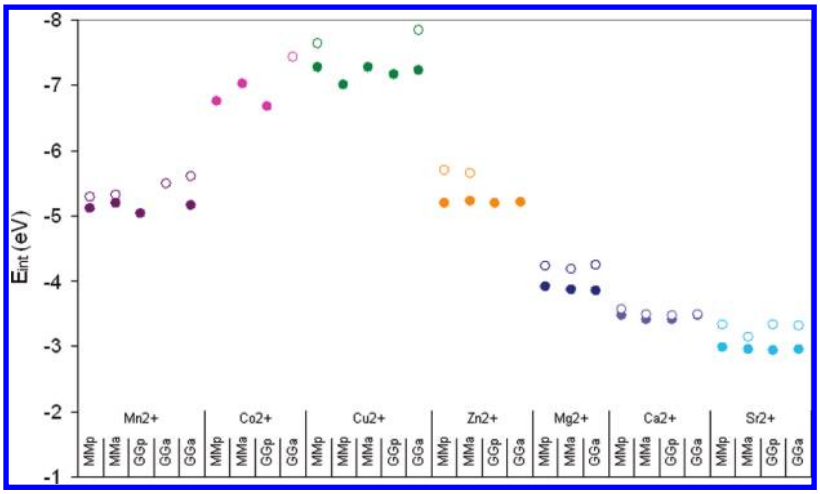

Figure 9. Interaction energies, E_{int}, of cations in the disaccharide 2-DC complexes. The interaction energies are obtained from the E_{int} equation in Section 3.1. E_{int} values in the complexes with water molecules in the first coordination shell are indicated with unfilled circles. The indices "p" and "a" denote, respectively, the parallel and antiparallel orientations of the disaccharide units.

hydroxyl oxygen in the GG or MM units. Note that the bidentate chelating binding type is formed when water is completely removed. The interaction energies of the cations increases in the hydrated complexes compared with the respective water-free structures, following the same order as that in the unhydrated complexes, that is, E_{int} (Cu^{2+}) > E_{int} (Co^{2+}) > E_{int} (Zn^{2+}) > E_{int} (Mn^{2+}).

DISCUSSION

The DFT structural and energetic results allowed us to distinguish between the complexation of the alkaline earth and of the TM cations. In a first place, one notices that the TMs form significantly shorter bonds with the diuronate oxygens. This suggested a different type of chemical binding depending on the chemical nature of the metal.

Looking closely at the molecular orbital compositions of the computed complexes, we found that the complexation of the alkaline earth metal ions is only due to electrostatic interaction between the divalent cation and the negatively charged uronate units. The results showed that there is not any overlap between alkaline earth cations and oxygen orbitals. Indeed, the cation orbitals remain localized around the cation center and do not extend to the ligands orbitals, which are also well-localized on the ligands. Moreover, the optimized ionic bond distances in the complexes are of very comparable lengths with those in the ionic oxide solids, equal to 2.106, 2.406, and 2.770 Å in the MgO, CaO, and SrO ionic crystals. Previous force-field calculations on the gelation process of Ca^{2+} with guluronate alginates[24] also concluded to the electrostatic interactions between Ca^{2+} and G-homopolymers.

In contrast, in all TM-containing complexes, a covalent bond formation between the TM center and uronate binding oxygens is clearly revealed from the molecular orbital analysis. Zn^{2+} ion forms minimum energy structures with closed electronic shells, whereas the complexes with the other TM ions have open-shell electronic structures as follows: high spin for the Mn^{2+} complexes (five unpaired 3d electrons located at the Mn^{2+} center) and low spin for the Co^{2+} and Cu^{2+} complexes (one unpaired 3d electron at the Co^{2+} and Cu^{2+}centers). In all cases, the TM 3d orbitals overlap with the valence orbitals of the ligands, which have predominantly O_{2p} character. Selected representative valence orbitals, illustrating this overlap, are shown in Figure 8. Similarly, covalent bonds are formed in the hydrated TM−disaccharide(s) structures and in the structures with one disaccharide.

The strong covalent-coordination TM−uronate bonds are also characterized with the higher E_{int} values compared with those of the alkaline-earth cations. A graphical comparison between E_{int} is presented in Figure 9 for the dry and hydrated complexes. The binding strength clearly depends on the nature of the metal cation, following the order Cu^{2+} > Co^{2+} > Zn^{2+} > Mn^{2+} ≫ Mg^{2+} > Ca^{2+} > Sr^{2+}. This tendency is also valid for the structures with one diuronate chain (Figure SI2.1 in the Supporting Information).

By considering the ionic radius of the cations, being often proposed to explain the stability orders in various metal cation complexes,[42] we note that the increasing ionic radius from Mg^{2+} to Ca^{2+} to Sr^{2+} indeed correlates with the decrease in complexation energies of alkaline earth cation-diuronates. This confirms again their ionic character of binding. The variation of E_{int} in the TM complexes does not correlate with the inverse of the TM ionic radius size of the metal cations: 0.97 Å (high-spin) for Mn, 0.79 Å (low spin) for Co, 0.87 Å for Cu, and 0.88 Å for Zn.[43] Instead, the increased stabilization is due to the 3d-O_{2p} covalent bond formations and depends on the particular electronic structure of the 3d cation. This also explains that the energy trend we obtained for the TM−disaccharide complexes for Mn, Co and Cu is often respected in their complexes with many other ligands and geometries.[42,43]

It is now interesting to relate E_{int} to the order of alginate affinities toward various divalent cations. The experimentally established affinities[44] follow the order: Cu^{2+} > Sr^{2+} > Ca^{2+} > Co^{2+} > Zn^{2+} > Mn^{2+}. Note that in other works,[45] the affinity of alginates toward Zn^{2+} is reported to be equal to that toward Co^{2+}. We found, however, that Zn^{2+} coordination resembles the coordination of Mn^{2+} (five coordination bonds), and its interaction energy is only slightly higher than E_{int} of Mn^{2+}. Despite it, the computed E_{int} trend for the studied TM series is comparable to the alginate affinity trend. Moreover, the E_{int} trend is respected for the GG or MM isomers for the dry or hydrated complexes with one or two diuronates. It emerges thus a conclusion that the formation of covalent-coordination bonds between the TM cations and uronate units plays a preponderant role in the processes of alginate gelation.

An inverse relation between alginate affinities and E_{int} in the alkaline earth series is obtained. The interactions of Ca^{2+} and Sr^{2+} disaccharide complexes are significantly smaller than E_{int} of the TM cations. Moreover, in the presence of Mg^{2+},the gelation is not observed because of the high solubility of Mg^{2+} alginate complex in water. All of these factors suggest that the alginate gelation in the presence of alkaline earth metals is not or is very little related to the $M^{2+}\cdots O$ binding strength. To estimate qualitatively the effect of ion hydration, we have also computed the interaction energies in the considered complexes by replacing the energy of the isolated cation with the energy of the cation octahedral aqueous complex in the equation in Section 3.1. The results presented in section SI4 in the Supporting Information demonstrate that these new E_{int} values, noted as E'_{int}, respect the same order for Cu^{2+}, Co^{2+}, and Mn^{2+}. The Zn^{2+} in $Zn^{2+}(H_2O)_6$ has nearly the same energy as Co^{2+} in the octahedral aqueous complex (see SI4 in the Supporting Information), which decreases significantly its E'_{int}. Similarly, magnesium cation in $Mg^{2+}(H_2O)_6$ interacts with water significantly stronger (by 0.2 eV) than Ca^{2+} and Sr^{2+}. This results in a stronger decrease in Mg^{2+} interaction energy in the disaccharide complexes. The relative stability trend computed by considering the cation octahedral aqueous complex as a reactant becomes: $Cu^{2+} > Co^{2+} > Mn^{2+} \geq Zn^{2+} \gg Ca^{2+} > Sr^{2+} > Mg^{2+}$.

It is worth noting that besides the cation−uronate complexation the gelation processes involves several other factors such as entropy, ion hydration, accessibility of uronate oxygens to the cations in the long alginate chain conformations, cooperative interactions, and long-range electrostatic interactions in the polyelectrolyte solutions. Nevertheless, we focused only on the cation−uronate complexation in this study; our results showed that the formation of covalent bonding has an important impact on the gelation of alginates in the presence of TMs. The widely accepted picture in the literature for the alginate gelation as a process driven mainly by the long-range electrostatic interactions seems to hold up to a largest extent only for the alkaline earth ions. For the TM cations, it appears to be very likely to conclude that the long-range electrostatic interactions in the polyelectrolyte solutions are competing with the TM cation−uronate chemical binding. The latter appear to have an important effect. These lead to the conclusion that two different types of interactions at the electronic level (due to the chemical nature of cations) bring a very similar macroscopic result that is the alginate gel formation in the presence of metal cations.

Further on, comparing E_{int} values in the GG and in MM complexes for a given cation, we note that they are of very similar stability order and depend on the particular geometry arrangements between the chain orientations and the type of binding. Therefore, it is not possible to attribute a clear preference of the metal complexations to a MM or GG block. This result is not surprising because the studied complexes are representative for the alginate solutions with an excess of gelling ions, and it is well established experimentally that in such a case each M or G uronate unit participates to the complexation. The E_{int} values do not give also a preference for a particular binding type in the TM−diuronates. Nevertheless, the present calculations favor the unidentate more than the bidentate chelating bonding; both types are predicted to give rise to stable complexes within a relatively small energy window, which is <1 eV for Mn^{2+} and Zn^{2+} and <1.5 eV for Co^{2+} and Cu^{2+}. This shows that in a first step of alginate gelation either binding type would be possible, and most probably at room temperature both binding types coexist in the gels.

CONCLUSIONS

In the present study, we focused on the complexation of disaccharide units to several TM and alkaline earth divalent cations by applying the quantum chemical DFT computational method. The DFT structural and energetic results were computed for a large number of possible metal−diuronate complexes with guluronate and mannuronate isomers, with one and two diuronates, and with and without water molecules in the inner coordination shells. In all complexes with TM cations, the bidentate and unidentate binding types can be present. The unidentate binding always leads to slightly more-stable structures.

For all studied structures, the molecular orbital analysis revealed that strong coordination-covalent bonds are formed in the TM complexes, whereas only ionic interaction occurs between the alkaline earth cations and the diuronates. The presence of water in the inner coordination shell does not change the above conclusions. The metal cations link either to the COO^- or to the hydroxyl oxygens, offering a large variety of stable hydrated or water-free structures. The order of cation bond strength to the uronate oxygens remains the same independently of the particular complex structure, number of water molecules, or one or two disaccharides considered in the complex.

There is a good correlation between the alginate affinity trend toward TM cation and the interaction energies of the TM cations. An inverse stability order is found for the alginate affinity and alkaline earth cation interaction energies. We thus conclude that the mechanism of alginate gelation in the presence of TM cations differs substantially from that in the presence of alkaline earth. The formation of covalent bonds in the alginate gels with TM cation seems to be preponderant over the electrostatic interactions in the polyelectrolyte solutions.

ASSOCIATED CONTENT

Supporting Information

Structural parameters of studied complexes with one disaccharide unit (1-DC). Interaction energies of studied cations in complexes with one disaccharide unit (1-DC). Interaction energies and bond distances of studied cations in complexes with two disaccharide units (2-DC). Graphical presentation of interaction energies in the 2-DC optimized cation-diuronate complexes, calculated using cation/aqueous complexes as a reactant. This material is available free of charge via the Internet at http://pubs.acs.org.

AUTHOR INFORMATION

Corresponding Author

*E-mail: tzonka.mineva@enscm.fr. Fax: (33) 4 67 16 34 70.

Notes

The authors declare no competing financial interest.

REFERENCES

(1) Barbotin, J. N.; Nava Saucedo, J. E. In *Polysaccharides*; Dumitriu, S., Ed.; Marcel Dekker: New York, 1998; p 749.

(2) Sime, W. J. In *Food Gels*; Harris, P., Ed.; Elsevier: Amsterdam, 1990; p 53.

(3) Chen, J. P.; Hong, L.; Wu, S.; Wang, L. *Langmuir* **2002**, *18*, 9413−9421.
(4) Haug, A. *Acta Chem. Scand.* **1959**, *13*, 1250−1251.
(5) Haug, A.; Smisrod, O. *Acta Chem. Scand.* **1965**, *19*, 341−351.
(6) Haug, A.; Smisrod, O. *Acta Chem. Scand.* **1965**, *19*, 329−340.
(7) Jang, K.; Nguyen, D; Geesey, G. G. *Water Res.* **1995**, *29*, 315−321.
(8) Grasdalen, H.; Anthonsen, T.; Larsen, B.; Smidsrod, O. *Acta Chem. Scand., Ser. B* **1975**, *29*, 99−108.
(9) Cesàro, A.; Crescenzi, V.; Delben, F.; Gamini, A.; Liut, G.; Paoletti, S.; Rizzo, R. *Thermochim. Acta* **1992**, *199*, 1−15.
(10) Wang, Z.-Y.; White, J. W.; Konno, M.; Saito, S.; Nozawa, T. *Biopolymer.* **1995**, *35*, 227−238.
(11) Zheng, H. *Carbohydr. Res.* **1997**, *302*, 97−101.
(12) Grant, G. T.; Morris, E. R.; Rees, D. A.; Smith, P. J. C. *FEBS Lett.* **1973**, *32*, 195−197.
(13) Morris, E. R.; Rees, D. A.; Thorn, D.; Boyd, J. *Carbohydr. Res.* **1978**, *66*, 145−154.
(14) Morris, E. R.; Rees, D. A.; Young, G. *Carbohydr. Res.* **1982**, *108*, 181−195.
(15) Cesàro, A.; Delben, F.; Paoletti, S. *J. Chem. Soc., Faraday Trans. 1* **1988**, *84*, 2573−2584.
(16) Ouwerx, C.; Velings, N.; Mestdagh, M. M.; Axelos, M. A. V. *Polym. Gels Networks* **1998**, *6*, 393−408.
(17) Khon, R. *Pure Appl. Chem.* **1975**, *42*, 371−397.
(18) Atkins, E. D. T.; Nieduszynski, I. A.; Mackie, W.; Parker, K. D.; Smolko, E. E. *Biopolymers* **1973**, *12*, 1879−1887.
(19) Mackie, W.; Perez, S.; Rizzo, R.; Taravel, F.; Vignon, M. *Int. J. Biol. Macromol.* **1983**, *5*, 329−341.
(20) Steginsky, C. A.; Beale, J. M.; Floss, H. G.; Mayer, R. M. *Carbohydr. Res.* **1992**, *225*, 11−26.
(21) Haug, A.; Smidsrod, O. *Acta Chem. Scand.* **1970**, *24*, 843−854.
(22) Kohn, R.; Larsen, B. *Acta Chem. Scand.* **1972**, *26*, 2455−2468.
(23) deRamos, C. M.; Irwin, A. E.; Nauss, J. L.; Stout, B. E. *Inorg. Chim. Acta* **1997**, *25*, 669−675.
(24) Braccini, I.; Perez, S. *Biomacromolecules* **2001**, *2*, 1089−1096.
(25) Fuks, L.; Filipiuk, D.; Majdan, M. *J. Mol. Struct.* **2006**, *792*−*793*, 104−109.
(26) Papageorgiou, S. K.; Kouvelos, E. P.; Favvas, E. P.; Sapalidis, A. A.; Romanos, G. E.; Katsaros, F. K. *Carbohydr. Res.* **2010**, *345*, 469−473.
(27) Nakamoto, K. *Infrared Spectra of Inorganic and Coordination Compounds*; Wiley: New York, 1997.
(28) Nara, M.; Torii, H.; Tasumi, M. *J. Phys. Chem.* **1997**, *100*, 19812−19817.
(29) Braccini, I.; Grasso, R. P.; Perez, S. *Carbohydr. Res.* **1999**, *317*, 119−130.
(30) Chen, J. P.; Wang, L.; Wu, Sh.; Hong, L. *Langmuir* **2002**, *18*, 9413.
(31) Agulhon, P.; Robitzer, M.; David, L.; Quignard, F. *Biomacromolecules* **2012**, *13*, 215−220.
(32) Tomasi, J.; Mennucci, B.; Cammi, R. *Chem. Rev.* **2005**, *105*, 2999−3093.
(33) Perdew, J. P.; Burke, K.; Ernzerhof, M. *Phys. Rev. Lett.* **1996**, *77*, 3865−3868.
(34) Frisch, M. J.; Trucks, G. W.; Schlegel, H. B.; Scuseria, G. E.; Robb, M. A.; Cheeseman, J. R.; Scalmani, G.; Barone, V.; Mennucci, B.; Petersson, G. A.; Nakatsuji, H.; Caricato, M.; Li, X.; Hratchian, H. P.; Izmaylov, A. F.; Bloino, J.; Zheng, G.; Sonnenberg, J. L.; Hada, M.; Ehara, M.; Toyota, K.; Fukuda, R.; Hasegawa, J.; Ishida, M.; Nakajima, T.; Honda, Y.; Kitao, O.; Nakai, H.; Vreven, T.; Montgomery, J. A., Jr.; Peralta, J. E.; Ogliaro, F.; Bearpark, M.; Heyd, J. J.; Brothers, E.; Kudin, K. N.; Staroverov, V. N.; Kobayashi, R.; Normand, J.; Raghavachari, K.; Rendell, A.; Burant, J. C.; Iyengar, S. S.; Tomasi, J.; Cossi, M.; Rega, N.; Millam, N. J.; Klene, M.; Knox, J. E.; Cross, J. B.; Bakken, V.; Adamo, C.; Jaramillo, J.; Gomperts, R.; Stratmann, R. E.; Yazyev, O.; Austin, A. J.; Cammi, R.; Pomelli, C.; Ochterski, J. W.; Martin, R. L.; Morokuma, K.; Zakrzewski, V. G.; Voth, G. A.; Salvador, P.; Dannenberg, J. J.; Dapprich, S.; Daniels, A. D.; Farkas, Ö.; Foresman, J. B.; Ortiz, J. V.; Cioslowski, J.; Fox, D. J. *Gaussian 09*, revision A.1; Gaussian, Inc.: Wallingford, CT, 2009.
(35) Köster, A. M.; Calaminici, P.; Casida, M. E.; Flores-Moreno, R.; Geudtner, G.; Goursot, A.; Heine, T.; Ipatov, A.; Janetzko, F.; Martin del Campo, J.; Patchkovskii, S.; Reveles, J. U.; Salahub D. R.; Vela A. *deMon2k*; The deMon Developers: Cinvestav, Mexico, 2006
(36) Geudtner, G.; Calaminici, P.; Carmona-Espíndola, J.; del Campo, J. M.; Domínguez-Soria, V. D.; Moreno, R. F.; Gamboa, G. U.; Goursot, A.; Köster, A. M.; Reveles, J. U.; Mineva, T.; Vásquez-Pérez, J. M.; Vela, A.; Zúñinga-Gutierrez, B.; Salahub, D. R. *Wiley Interdiscip. Rev.: Comput. Mol. Sci.* **2011**, DOI: DOI: 10.1002/wcms.98.
(37) Godbout, N.; Salahub, D. R.; Andzelm, J.; Wimmer, E. *Can. J. Chem.* **1992**, *70*, 560−571.
(38) Calaminici, P.; Janetzko, F.; Köster, A. M.; Mejia-Olvera, R.; Zuñiga-Gutierrez, B. *J. Chem. Phys.* **2007**, *126*, 044108−044118.
(39) Wu, Q.; Yang, W. *J. Chem. Phys.* **2002**, *116*, 515−524.
(40) Reveles, J. U.; Köster, A. M. *J. Comput. Chem.* **2004**, *25*, 1109−1116.
(41) Dheu-Andries, M.; Perez, S. *Carbohydr. Res.* **1983**, *124*, 324−332.
(42) Irving, H.; Williams, R. J. P. *J. Chem. Soc.* **1953**, *8*, 3192−3210.
(43) Shannon, R. D. *Acta Crystallogr.* **1976**, *A32*, 751−767.
(44) Rezaii, N.; Khodagholi, F. *Protein J.* **2009**, *28*, 124−30.
(45) Ma, P. X. In *Alginate for Tissue Engineering. In Scaffolding in Tissue Engineering*; Ma, P. X., Elisseeff, J., Eds.; CRC Press, Taylor and Francis Group: Boca Raton, FL, 2006; p 14.